Available online at www.sciencedirect.com
ScienceDirect
Journal of Power Sources 160 (2006) 846–851
JOURNAL OF POWER SOURCES
www.elsevier.com/locate/jpowsour

Short communication

Molten Carbonate Fuel Cell electrochemistry modelling

Sergio Bittanti [a], Silvia Canevese [a,*], Antonio De Marco [a], Antonio Errigo [b], Valter Prandoni [c]

[a] *Dipartimento di Elettronica e Informazione, Politecnico di Milano, Piazza Leonardo da Vinci 32, 20133 Milan, Italy*
[b] *CESI S.p.A., Via R. Rubattino 54, 20134 Milan, Italy*
[c] *CESI RICERCA S.p.A., Via R. Rubattino 54, 20134 Milan, Italy*

Available online 5 July 2006

Abstract

A Fuel Cell (FC) is an electrochemical device which produces electric energy in DC. In order to support design control for the electrical system connected to it, it is necessary to work out a suitable representation of the fast dynamics involved. Therefore, in this work, a mathematical model, based on first principles and including both dynamical equations and algebraic relations, is described for electrochemical reactions, with the related formation of potential differences and anion and cation accumulation phenomena, in a Molten Carbonate Fuel Cell (MCFC). The model is formally consistent and it has been validated against experimental results, such as steady-state power and voltage versus current curves.

Keywords: MCFC; Dynamic mathematical model; Activated complex

1. Introduction

This work focuses on electrochemical reactions and on ionic transport inside a Molten Carbonate Fuel Cell (MCFC), so that the consequent production of potential differences across a cell and the electric current flowing inside it and through the external circuit connected to it can be calculated [1–5]. This discussion can be considered as a refinement of the electrical description, based on the Nernst equation, presented in [6,7], and it is meant to analyze relatively fast dynamics (time scale around a second, at most) in the cell behaviour. This will help understand cell performance limits, especially when abrupt changes in the power requested by the user occur, as in emergency conditions (typically, either load loss or sudden increase in power request). Of course, this also influences the design of possible control systems, which, in fact, will have to be able to react to such fast and/or large "disturbances" in a proper way, guaranteeing power quality and flexibility while keeping device operation safe. We remark that, although, in the literature, there are various mathematically exhaustive models ([8–10], e.g.) for the electrochemical behaviour of a cell, those models hold, in general, for stationary conditions, i.e. they do not describe the dynamics of the electrochemical reactions at the electrodes and of the ionic components transport.

2. The model

The stratified structure of a single MCFC is reported in Fig. 1. Gas flows at the top and at the bottom are assumed to be in orthogonal directions with respect to each other and to the cell thickness: this cross flow, indeed, causes strong chemical coupling between corresponding anode and cathode points and therefore it requires to study the behaviour of each strip (indicated with a parallelepiped) along the cell thickness. The approach followed here is adapted to the three-phase electrochemical structure of each strip: the gases (i.e. the anodic and the cathodic feeding mixtures) and the liquid (i.e. the electrolyte) involved can react only in the presence of the solid electrode material. This last acts as a catalyst, offering empty sites to which gas molecules can attach and form activated complexes, which, in turn, react with the electrolyte ions. Since there are charged activated sites, a surface charge distribution originates on each cell

* Corresponding author. Tel. +39 0223993467; fax: +39 0223993412.
E-mail addresses: bittanti@elet.polimi.it (S. Bittanti), canevese@elet.polimi.it (S. Canevese), demarco@mail2.elet.polimi.it (A. De Marco), errigo@cesi.it (A. Errigo), prandoni@cesiricerca.it (V. Prandoni).

0378-7753/$ – see front matter © 2006 Elsevier B.V. All rights reserved.
doi:10.1016/j.jpowsour.2006.04.057

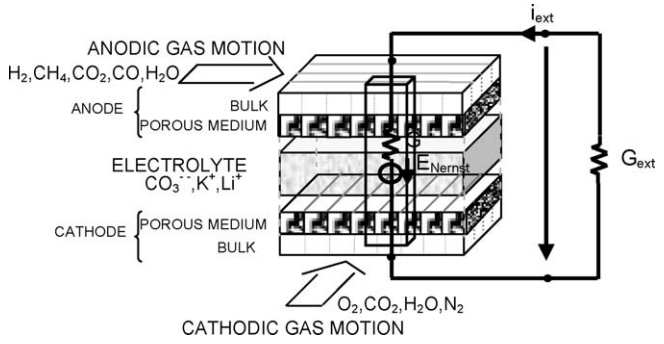

Fig. 1. The considered MCFC structure.

electrode, so that a potential difference arises and a capacitive effect is highlighted. That potential difference, together with the fact that carbonate ions are consumed or produced by reactions, is responsible of ionic movement inside the cell. The mathematical model studies three separated zones, both at the anode and at the cathode (as summarized in Fig. 2, where the spatial x coordinate associated to each of them is shown too): the first, called the Helmholtz layer (compare [11]), is the one where the electrochemical reactions take place and it is part of charged materials; the second is the electrolyte zone, inside a pore, in which electroneutrality cannot be assured (i.e. it is a space charge region), since anions tend to accumulate near the anode to decrease near the cathode; the last one, which is called here the (electrolyte) axial region and which connects the anode and cathode cell sides, is that in which electroneutrality can be assumed.

2.1. The Helmholtz layers

The reaction mechanism, described below by formulae (1)–(3) at the anode, and (4)–(6) at the cathode, has been split into sub-reaction steps which lead to the formation of activa ted complexes ($MHCO_3^{--}$ and MOH^- at the anode, MO^- and MCO_3^{--} at the cathode) which, in turn, give rise to potential barriers, described by their peak values E_{pa} and E_{pc}. M is a free metal site.

More specifically, the hypothesized mechanism at the anode is

$$\frac{1}{2}H_2 + M \underset{\dot r_{-1}}{\overset{\dot r_1}{\rightleftarrows}} MH, \text{ with } \dot r_1 \gg \dot r_{-1} \text{ (and therefore negligible)} \tag{1}$$

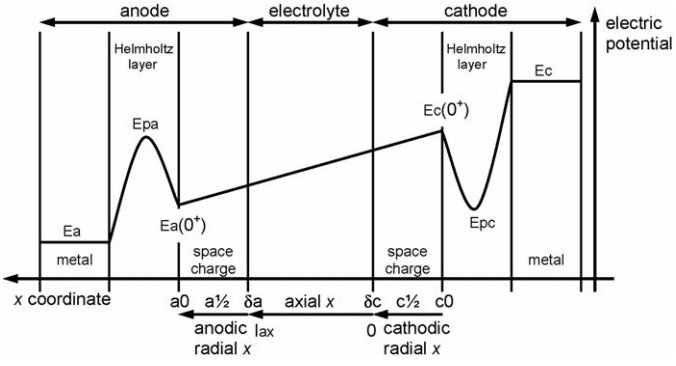

Fig. 2. The adopted Cartesian coordinates and the potential profile along a cell.

$$MH + CO_3^{--} \underset{\dot r_{-2}}{\overset{\dot r_2}{\rightleftarrows}} MHCO_3^{--} \rightleftarrows CO_2 + e + MOH^- \tag{2}$$

$$MOH^- + H_2 \underset{\dot r_{-2b}}{\overset{\dot r_{2b}}{\rightleftarrows}} H_2O + e + MH, \tag{3}$$

and at the cathode

$$\frac{1}{2}O_2 + M \rightleftarrows \frac{1}{2}M_2O_2 \tag{4}$$

(very fast, therefore negligible: there will always be M_2O_2 sites)

$$\frac{1}{2}M_2O_2 + e \underset{\dot r_{-3}}{\overset{\dot r_3}{\rightleftarrows}} MO^- \tag{5}$$

$$MO^- + CO_2 + e \underset{\dot r_{-4}}{\overset{\dot r_4}{\rightleftarrows}} MCO_3^{--} \rightleftarrows CO_3^{--} + M. \tag{6}$$

$\dot r_2$ and $\dot r_{-2}$ are supposed to be a fast and a slow step, respectively, $\dot r_{2b}$ a fast one too; similarly, $\dot r_3$ and $\dot r_{-4}$ are supposed to be fast steps, while $\dot r_4$ a slow one.

Dynamic equations are based on Butler-Volmer-like reaction rates, and on the Planck-Nernst formula for charged species fluxes. In particular, for the anodic rates one can write

$$\dot r_2 = K_2 C^-_{a0}(1 - \theta_a - \theta_{act}) e^{-((E_{pa} - E_a)/RT)F} \tag{7}$$

$$\dot r_{-2} = K_{-2} C_{CO_2 a0} \theta_a e^{-((E_{pa} - E_a(0^+))/RT)F} \tag{8}$$

$$\dot r_{2b} = K_{2b} C_{H_2 a0} \theta_a e^{-(1+\beta_{a\varepsilon})((E_a(0^+) - E_a)/RT)F} \tag{9}$$

$$\dot r_{-2b} = K_{-2b} C_{H_2 O a0}(1 - \theta_a - \theta_{act}) e^{-\beta_{a\varepsilon}((E_a(0^+) - E_a)/RT)F}, \tag{10}$$

where θ_a, θ_{act} and $1 - \theta_a - \theta_{act}$ are the surface fractions occupied, respectively, by MOH^-, by $MHCO_3^{--}$ and by the H_2 molecules tied to the electrode, the K_i's are temperature-dependent coefficients and the concentrations involved are those at the electrode–electrolyte interface. Superscript ($^-$) stands for the carbonate anion. According to analogous definitions, for the cathode one can write

$$\dot r_3 = K_3 C^{1/2}_{O_2 c0}(1 - \theta_c - \theta_{c_{act}}) e^{-(1+\beta_{c\varepsilon})((E_c - E_c(0^+))/RT)F} \tag{11}$$

$$\dot r_{-3} = K_{-3} \theta_c e^{-\beta_{c\varepsilon} \frac{E_c - E_c(0^+)}{RT} F} \tag{12}$$

$$\dot r_4 = K_4 C_{CO_2 c0} \theta_c e^{-\frac{E_c - E_{pc}}{RT} F} \tag{13}$$

$$\dot r_{-4} = K_{-4} C^-_{c0}(1 - \theta_c - \theta_{c_{act}}) e^{-\frac{E_c(0^+) - E_{pc}}{RT} F}. \tag{14}$$

Letting T_a and T_{act} be the number of anodic sites moles of the two possible kinds per unit area, the conservation equations of the occupied sites are then

$$T_a \frac{d\theta_a}{dt} = \dot r_2 - \dot r_{-2} - \dot r_{2b} + \dot r_{-2b} \tag{15}$$

$$T_{act} \frac{d\theta_{act}}{dt} = z^- J^-_{a0} - (\dot r_2 - \dot r_{-2}), \tag{16}$$

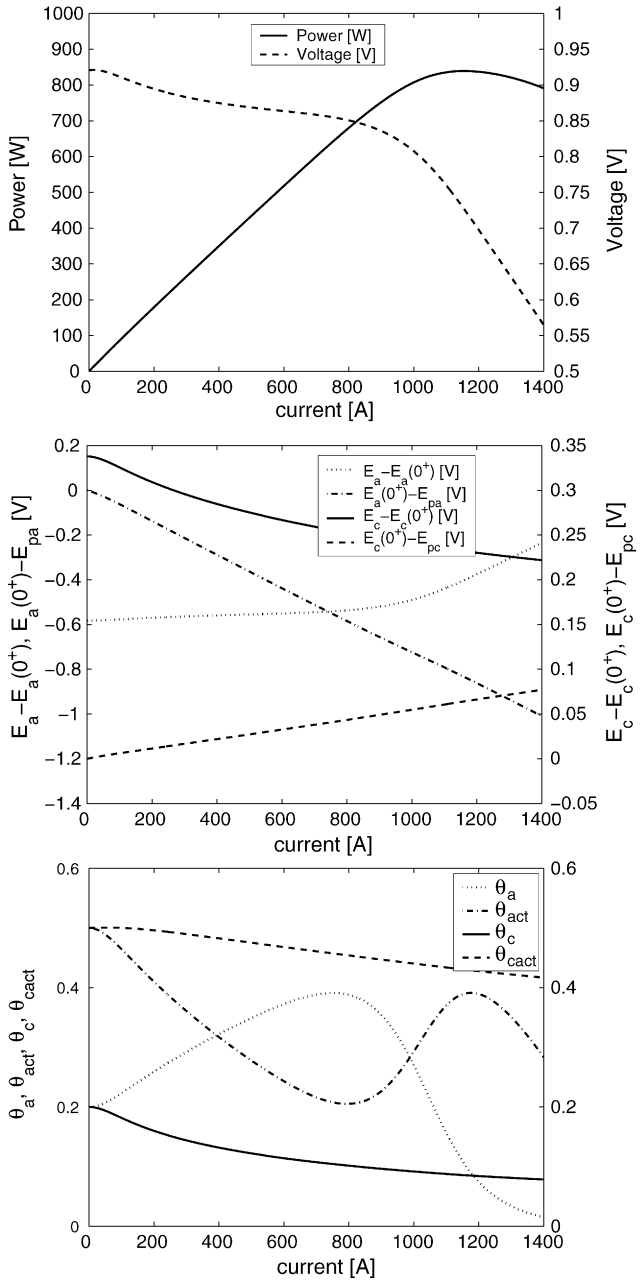

Fig. 3. From top to bottom: power and voltage vs. current: simulated behaviour of a single cell with 700 about 0.8 m^2 area; electrode potential differences; electrode surface fraction occupied by activated sites, both at the anode ($\theta_a := \mathrm{MOH}^-$, $\theta_{act} := \mathrm{MHCO}_3^{--}$) and at the cathode ($\theta_c := MO^-$, $\theta_{cact} := \mathrm{MCO}_3^{--}$).

where the anion flux at the a0 interface is, for the Planck-Nernst formula,

$$J_{a0}^- = -\upsilon^- z^- F C_{a0}^- \frac{E_{pa} - E_a(0^+)}{l_{hza}} - D^- \frac{dC^-}{dR}. \quad (17)$$

R is the anodic radial x, l_{hza} the Helmholtz layer width and υ^-, z^- and D^- are CO_3^{--} mobility, number of charges and diffusion coefficient, respectively.

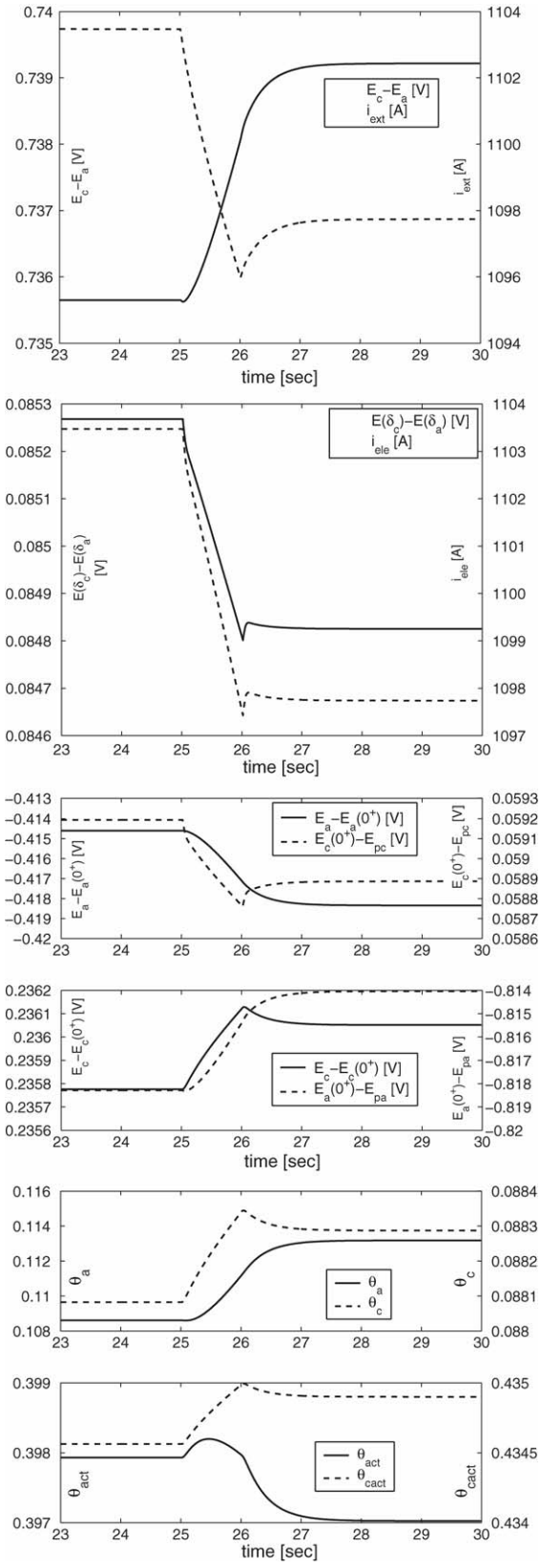

Fig. 4. G_{ext} from 1500 S to 1485 S in 1 s: from top to bottom: external voltage and current, electrolyte voltage and current, electrode potential differences, the θ variables.

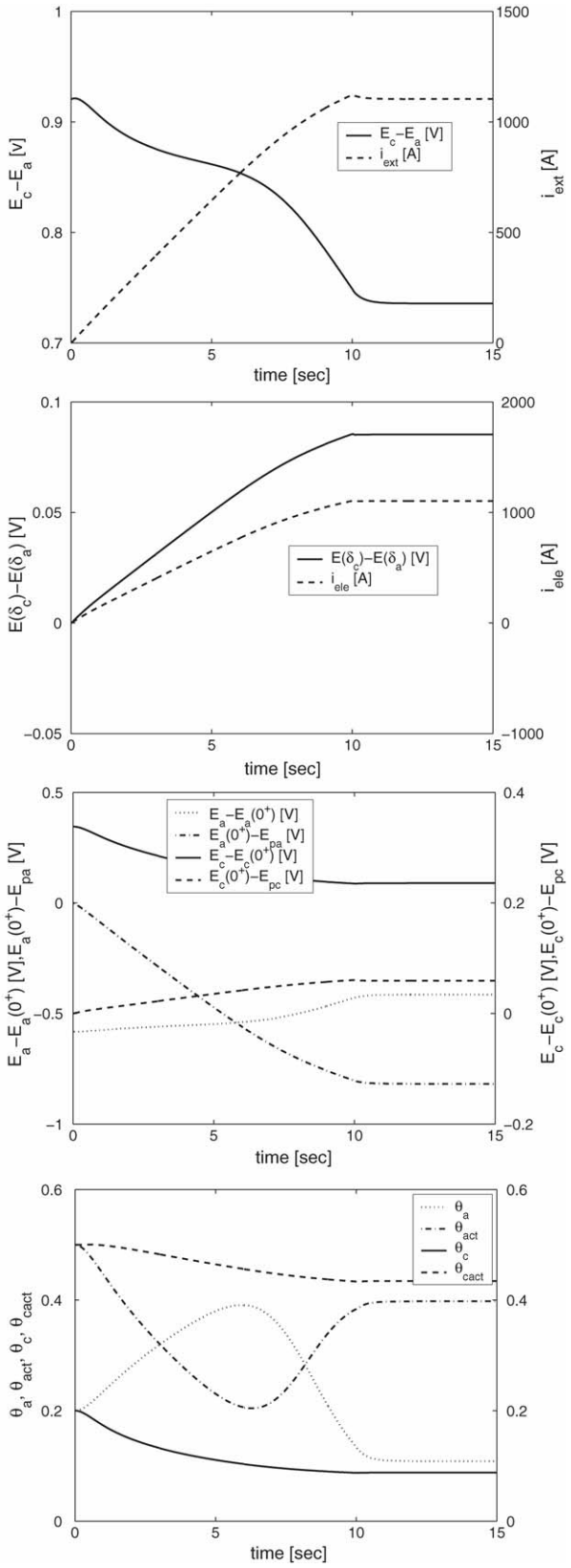

Fig. 5. G_{ext} from 0 S to 1500 S in 10 s: from top to bottom: external voltage and current, electrolyte voltage and current, electrode potential differences, the θ variables.

The anodic external current, i_a, will be given by

$$\frac{i_a}{FS_{\text{ra}}} = \dot{r}_2 - \dot{r}_{-2} + \dot{r}_{2b} - \dot{r}_{-2b}, \tag{18}$$

where S_{ra} is the anodic reaction surface. As for the potential difference $E_a(0^+) - E_a$, the classical Coulomb relation supplies

$$E_a(0^+) - E_a = -\frac{\sigma_{\text{hza}}}{2\varepsilon_{\text{hza}}} l_{\text{hza}}, \tag{19}$$

with the surface charge [Cm^{-2}] in the Helmholtz layer

$$\sigma_{\text{hza}} = T_{\text{act}}\theta_{\text{act}} F z_{\text{MHCO}_3^{--}} + T_a\theta_a F z_{\text{MOH}^-}. \tag{20}$$

As before, for the cathode one has

$$T_c \frac{\mathrm{d}\theta_c}{\mathrm{d}t} = \dot{r}_3 - \dot{r}_{-3} - \dot{r}_4 + \dot{r}_{-4} \tag{21}$$

$$T_{c_{\text{act}}} \frac{\mathrm{d}\theta_{c_{\text{act}}}}{\mathrm{d}t} = -z^- J_{c0}^- + (\dot{r}_4 - \dot{r}_{-4}) \tag{22}$$

$$J_{c0}^- = -\upsilon^- z^- F C_{c0}^- \frac{E_{\text{pc}} - E_c(0^+)}{l_{\text{hzc}}} - D^- \frac{\mathrm{d}C^-}{\mathrm{d}R}. \tag{23}$$

The potential difference $E_c - E_c(0^+)$ can be written as

$$E_c - E_c(0^+) = -\frac{\sigma_{\text{hzc}}}{2\varepsilon_{\text{hzc}}} l_{\text{hzc}}, \tag{24}$$

where

$$\sigma_{\text{hzc}} = T_{c_{\text{act}}}\theta_{c_{\text{act}}} F z_{\text{MCO}_3^{--}} + T_c\theta_c F z_{\text{MO}^-}, \tag{25}$$

and the cathodic external current as

$$\frac{i_c}{FS_{\text{rc}}} = \dot{r}_3 - \dot{r}_{-3} + \dot{r}_4 - \dot{r}_{-4}. \tag{26}$$

Notice that the proposed equations have a correct stationary limit with no current: in fact, few mathematical manipulations lead to the classical thermodynamical Nernst equation, both at the anode and at the cathode of course:

$$\frac{E_a - E_a(0^+)}{RT} 2F = \ln \frac{K_{-2}K_{-2b}}{K_2 K_{2b}} + \ln \frac{C_{\text{CO}_2\text{a}0} C_{\text{H}_2 O\text{a}0}}{C_{\text{a}0}^- C_{\text{H}_2\text{a}0}} \tag{27}$$

$$\frac{E_c - E_c(0^+)}{RT} 2F = \ln \frac{K_3 K_4}{K_{-3} K_{-4}} + \ln \frac{(C_{\text{O}_2 c0})^{(1/2)} C_{\text{CO}_2 c0}}{C_{c0}^-}. \tag{28}$$

2.2. The space charge regions

In these zones, mass conservation equations for charged species, both negative and positive, are considered:

$$\frac{\partial C^\pm}{\partial t} + \frac{\partial J^\pm}{\partial x} = 0, \tag{29}$$

where, again, according to the Planck-Nernst formulation, the flux writes

$$J_a^\pm = -\upsilon^\pm z^\pm F C^\pm \frac{\partial \phi_a}{\partial R} - D^\pm \frac{\partial C^\pm}{\partial R}. \tag{30}$$

Notice that, again, superscript ($^-$) refers to the carbonate ion, while superscript ($^+$) refers to K^+ and Li^+, here considered together as forming a unique "equivalent" cation.

2.3. The axial model and closing equations

In that part of the electrolyte stretching from one electrode to the other, the mass conservation equation for a hypothesised average negative charge concentration (in fact, electroneutrality writes $2\overline{C^-}_{ax} = \overline{C^+}_{ax}$), namely

$$\frac{\partial \overline{C^-}_{ax}}{\partial t} + \frac{\partial J^-_{ax}}{\partial x_{ax}} = 0 \tag{31}$$

is integrated (from $x_{ax} = 0$ to $x_{ax} = l_{ax}$). Substituting the flux using the Nernst-Planck expression yields this state equation in the state variable $\overline{C^-}_{ax}$:

$$\dot{\overline{C^-}}_{ax} = -2\nu^- z^- F \overline{C^-}_{ax} \frac{E_c(\delta_c) - E_a(\delta_a)}{l^2_{ax}} - 2D^- \frac{\overline{C^-}_{ax} - C^-_{\delta_c}}{l^2_{ax}} + 2D^- \frac{C^-_{\delta_a} - \overline{C^-}_{ax}}{l^2_{ax}}. \tag{32}$$

Finally, the circuit is closed considering the Ohm law inside the electrolyte (this is part of the axial region indeed), i.e.

$$i_{ele} = \sigma_{ele} \frac{E_c(\delta_c) - E_a(\delta_a)}{l_{ax}} F S_{ax}, \tag{33}$$

the external electronic current

$$i_{ext} = (E_c - E_a) G_{ext} = i_c = i_a \tag{34}$$

and the Kirchhoff equation for potentials:

$$E_c - E_a = (E_c - E_c(0^+)) + (E_c(0^+) - E_c(\delta_c)) + (E_c(\delta_c) - E_a(\delta_a)) + (E_a(\delta_a) - E_a(0^+)) + (E_a(0^+) - E_a). \tag{35}$$

3. Simulation results

This section reports, first, some observations about parameter estimation, like that of the device internal resistance and of the thickness of the space charge regions, and then some simulation results obtained with the implemented model, focusing, in particular, on the stationary power versus current profile and on some dynamical characteristics. For simplicity, here, only an elementary MCFC, instead of a stack, is taken into account and only one instance (associated to the whole cell) for each electrochemical variable is employed. In other words, the elementary cell is considered as formed by a unique electrical strip (corresponding to the one at the anode and cathode inlet).

Cell internal resistance has been measured, at CESI, on a laboratory stack, through a short circuit experiment [12]: the average result, over those 14 cells with 700 cm^2 useful area each and over different hot time values, was 0.7 mΩ. The value obtained with a 1 μs short circuit simulation is 0.698 mΩ (this takes in the resistance of the anodic and cathodic metal plates and that of the electrolyte, but not that of the bipolar plate and of the gas distributor, which has not been included in the model yet, but which is presumably negligible). This agreement with the experimental value contributes to support model reliability (in conjunction with sound parameter calibration).

A simple estimate of δ_a and of δ_c can be obtained by linearly approximating the ion concentration Galerkin parabolas, built on the three concentrations C^-_{a0}, $C^-_{a\frac{1}{2}}$ and $C^-_{\delta a}$ and on C^-_{c0}, $C^-_{c\frac{1}{2}}$ and $C^-_{\delta c}$ respectively, at points a0 and $a\frac{1}{2}$ and at $c0$ and $c\frac{1}{2}$ respectively, and by determining the vanishing points of the two straight lines, all this with the passing of time: from this procedure, it appears that the approximation of assuming constant δ, $s = 10^{-8}$ m is rather a good one.

A relevant feature in the cell behaviour is the dependence of stationary power and voltage on current: model reliability is sustained by the comparison between simulated curves such as those shown at the top of Fig. 3 and characteristic curves found in the literature (compare, for example, [13]). The fact that, for increasing current values, power starts to decrease can be explained partly as a kinetic limit, partly as due to concentration polarization: in fact, for high current values, at the beginning the problem is that there are not enough activated sites to sustain the electrochemical reactions (as shown, again, in Fig. 3), but then, when they manage to be produced, the carbonate ion is not fast enough in moving, by diffusion most of all, from the anode side to the cathode side, to feed reactions again; therefore, the potential differences $E_a(0^+) - E_a$ and $E_c - E_c(0^+)$ (Fig. 3) decrease, causing the external potential difference $E_c - E_a$, and therefore power, to decrease. This explanation, anyway, could be checked and/or refined by modifying the model, in particular by inserting a more truthful pore distribution, instead of the uniform one adopted so far.

As already remarked, the model should be useful also to inquire cell dynamics; therefore, the variations exhibited by the electrochemical variables because of rather fast load variations are reported: Fig. 4 shows the case when G_{ext} decreases, from a stationary value equal to 1500 S, to 1485 S, in 1 s (the load starts to change at time $t = 25$ s here). Fig. 5 illustrates an example of a large load variation: it is assumed that G_{ext} increases from 0 S (at time $t = 0$ s) to 1500 S in 10 s and then sticks to the final value which it has attained.

4. Conclusions

A dynamical electrochemical model has been described to study the fast phenomena involved in the behaviour of a MCFC. Simulation results coming from its implementation show that it is able to reproduce some experimental facts like power decrease for high current values.

We remark that the model can be integrated with a thermo-fluid-dynamical model [5,6] of a MCFC, so as to obtain an overall dynamical description, valid for both low and relatively high frequencies, i.e. for time scales both on the order of an hour or tens of seconds and on the order of a second. This procedure is presented in [14].

Acknowledgements

This work has been developed in the frame of the research on the Italian Electrical System "Ricerca di Sistema", Min-

isterial Decrees of January 26, 2000 and April 17, 2001. Research has also been supported by the Italian National Research Project "New Techniques of Identification and Adaptive Control for Industrial Systems" and partially by CNR-IEIIT.

References

[1] C. Hamann, A. Hamnett, W. Vielstich, Electrochemistry, Wiley-VCH, Weinheim, Federal Republic of Germany, 1998.
[2] F. Goodridge, K. Scott, Electrochemical Process Engineering, Plenum Press, New York, 1995.
[3] V. Prandoni, A. De Marco, Modelli matematici dinamici delle reazioni elettrochimiche, catalitiche e trasferimenti di massa in celle a combustibile, CESI Internal Report A3/021830, Milan, Italy, 2003.
[4] A. Errigo, Modellistica delle reazioni elettrochimiche e del trasporto ionico in celle a combustibile, Master thesis, Politecnico di Milano, Milan, Italy, 2004.
[5] S. Canevese, Modelling and control of fuel cells, Ph.D. thesis, Politecnico di Milano, Milan, Italy, 2005.
[6] S. Canevese, A. De Marco, G. Moretti, V. Prandoni, Un Modello di Pila a Combustibile a Carbonati Fusi, ENERSIS, Milan, Italy, 2004.
[7] S. Bittanti, S. Canevese, A. De Marco, G. Moretti, V. Prandoni, Molten carbonate Fuel Cell Modelling, 16th IFAC World Congress, Prague, Czech Republic, 2005.
[8] C. Yuh, J. Selman, J. Electrochem. Soc. 131 (1984) 2062–2069.
[9] R. Peled, E. Gileadi, Electrochim. Acta 23 (1978) 361.
[10] M. Elam, E. Gileadi, J. Electrochem. Soc. 126 (1979) 1474.
[11] P. Belli, A. Ferretti, Modellistica e controllo di un impianto di riduzione selettiva catalitica (SCR) degli ossidi di azoto prodotti da una centrale termoelettrica, Master thesis, Politecnico di Milano, Milan, Italy, 1994–1995.
[12] M. Scagliotti, G. Strobino, P. Araldi, P. Savoldelli, Sperimentazione di una soluzione innovativa per la configurazione di stack MCFC, Giornata di studio sulle Pile a Combustibile, AIM, Milan, Italy, 1999.
[13] E.G.&G. Services, Parsons Inc., Fuel Cell Handbook (5th Edition), U.S. Dept of Energy, Off. of Fossil Energy, National Energy Technology Laboratory, Morgantown, West Virginia, 2000.
[14] S. Bittanti, S. Canevese, A. De Marco, A. Errigo, G. Giuffrida, V. Prandoni, Molten Carbonate Fuel Cell dynamical modelling, 1st EFC, Rome, Italy, 2005.